

# ANALYSIS OF PSS AND SSSC CONTROLLERS EFFECTS ON POWER SYSTEM OSCILLATIONS DAMPING

Marcelo S. Castro\*, Hugo M. Ayres<sup>†</sup>, Vivaldo F. da Costa<sup>‡</sup>, and Luiz C. P. da Silva<sup>§</sup>

School of Electrical and Computer Engineering  
University of Campinas (UNICAMP), Campinas, SP, Brazil

\* Email: mcastro@dsce.fee.unicamp.br

<sup>†</sup> Email: hmayres@dsce.fee.unicamp.br

<sup>‡</sup> Email: vivaldo@fee.unicamp.br

<sup>§</sup> Email: lui@fee.unicamp.br

**Abstract**—This paper investigates the performance of power system stabilizers (PSSs) and the static synchronous series compensator (SSSC) for damping undesirable power system low frequency oscillations. This study is carried out for both local and inter-area oscillations mode. The analysis and design of stabilizers, PSS and power oscillation damping (POD) controllers, are based on modal analysis, Hopf bifurcations, and time and frequency response techniques. The simulation results presented reveal a better effectiveness of the high power electronic based controller, namely, SSSC, than the PSS for damping power system low frequency electromechanical oscillations as well as for extend power systems small-signal stability limits. Furthermore, it is shown that PSSs and SSSC controllers could work together in an harmonious way to damp power system oscillations.

**Keywords**—Electromechanical Oscillations, Hopf bifurcations, PSS, POD, SSSC, Small-signal rotor angle stability.

## I. INTRODUCTION

Damping of electromechanical low frequency oscillations between interconnected synchronous generators is essential for secure system operation [1], [2]. In order to damp power system oscillations and enhance rotor angle stability, power system stabilizers (PSSs) have been successfully employed in many power systems worldwide [3]. Although in many instances, especially for critical inter-area oscillations, this solution is both inexpensive and effective, there are cases where the PSSs do not reach a suitable performance [2], then, other solutions must be sought.

Nowadays, due to technological stage of high power electronic controllers, another effective solution such as the use of flexible ac transmission systems (FACTS) is being considered [4], [5]. Even though the installation of FACTS controllers in power systems may not be justified just by its damping contribution, this is one the most suggested applications of these controllers as well as to the steady-state control of power flow and voltages [4], [5].

This paper investigates the effectiveness of PSSs and a series FACTS controller, namely, static synchronous series compensator (SSSC) for damping low frequency electromechanical oscillations and for extend power systems small-signal stability limits as well. The analysis is carried out for both local and inter-area oscillations modes. Two test systems, widely utilized in the literature for rotor angle stability studies, are considered in order to obtain the simulation results.

The paper is organized as follows: Section II introduces power system modeling and analysis concepts adopted in this paper; thus, the basic theory behind Hopf bifurcations and the used model of PSS are briefly discussed. In Section III the basic SSSC operation characteristics are described and the SSSC model for damping electromechanical oscillations is presented. Simulation results and discussion are presented in Sections IV and V. Section VI provides the main conclusions of the paper.

## II. BASIC BACKGROUND

### A. Power System Modeling

In general, power systems are modeled by a set of differential and algebraic equations (DAE), as follows:

$$\begin{aligned}\dot{x} &= f(x, y, \mu) \\ 0 &= g(x, y, \mu)\end{aligned}\quad (1)$$

where  $x$  is a vector of state variables associated with the dynamic states of generators, loads, and other system controllers;  $y$  is a vector of algebraic variables associated with steady-state variables resulting from neglecting fast dynamics (e.g., most load voltage phasor magnitudes and angles); and  $\mu$  is a set of uncontrollable parameters, such as variations in active and reactive power of loads (i.e., loading factor of the system).

For small-signal stability analysis (based on modal analysis), we assume that the system parameter variation is sufficiently small so that (1) can be linearized at an equilibrium point  $(x_o, y_o, \mu)$  as:

$$\begin{aligned}\Delta\dot{x} &= J_1\Delta x + J_2\Delta y + B\Delta u \\ 0 &= J_3\Delta x + J_4\Delta y\end{aligned}\quad (2)$$

where  $J_1$ ,  $J_2$ ,  $J_3$ , and  $J_4$  are Jacobian matrices of  $f$  and  $g$  related to the state and algebraic variables, respectively, and  $B$  is the perturbation matrix. If  $J_4$  is nonsingular, the vector of algebraic variables  $\Delta y$  in (2) can be eliminated which results in the state space representation as follows:

$$\Delta\dot{x} = (J_1 + J_2J_4^{-1}J_3)\Delta x + B\Delta u = \mathcal{A}\Delta x + B\Delta u \quad (3)$$

where  $\mathcal{A}$  is the system state matrix. Therefore, bifurcations on power system model can be detected by monitoring the eigenvalues of matrix  $\mathcal{A}$  as the loading factor  $\mu$  is increased.

### B. Hopf Bifurcations

Hopf bifurcations, also known as oscillatory bifurcations, are associated with a pair of purely imaginary eigenvalues of the state matrix  $\mathcal{A}$  [6]. In the dynamic system (1), when the parameter  $\mu$  varies, the equilibrium point  $(x_o, y_o, \mu)$  changes, and so do the eigenvalues of the corresponding system state matrix  $\mathcal{A}$  in (3). The point where a complex conjugate pair of eigenvalues reaches the imaginary axis due to the changes in  $\mu$ , is known as a Hopf bifurcation point [6] and defines the value of loading factor for which the system becomes unstable. In this paper, Hopf bifurcation theory is used to analyze the performance of PSS and SSSC controller for damping power system oscillations on two test systems, as shown in Sections IV and V.

### C. Power System Stabilizer

The function of a power system stabilizer (PSS) is to add damping to the generator rotor oscillations by excitation system using auxiliary stabilizing signals such as shaft speed, terminal frequency and/or power. The application of PSS has long been recognized as a very effective method for enhancing small-signal stability performance of the system [3]. Fig. 1 shows the structure of the model of a speed based PSS [1]. The phase compensation blocks provide the appropriate phase-lead characteristic to compensate for the phase lag between the exciter and the electrical torque of the generator. The washout control block is used to avoid affecting steady-state operation of the controller, and the stabilizer gain determines the amount of damping introduced by the PSS.

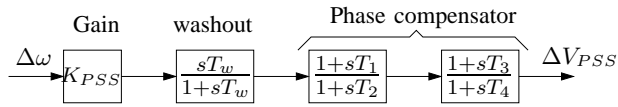


Fig. 1. PSS model used for simulations, where  $V_{PSS}$  is an additional input for the automatic voltage regulator.

## III. STATIC SYNCHRONOUS SERIES COMPENSATOR

The SSSC is a modern series FACTS controller based on voltage source converter (VSC) [4], [5]. The VSC is the basic electronic block of the SSSC, which by using gate-turn-off (GTO) thyristors converts an input dc voltage into a three-phase ac voltage at fundamental frequency. If the output ac voltage of the SSSC is always kept in quadrature with the line current, there is no active power exchange between the SSSC and the power system. When the SSSC voltage lags the line current by  $90^\circ$ , it works like a series capacitor, conversely, when its voltage leads the line current by  $90^\circ$  it works like a series inductor. Thus a SSSC can be considered as a series reactive compensation where the degree of compensation can be varied by controlling its output voltage [7], [8]. Even though oscillation control using SSSC is a costly option when compared to the use of PSSs, there are additional benefits of using this FACTS controller, such as an increase in system loadability and power flow control [4], [5], which is not possible at all with PSS.

### A. Transmission Characteristics

Fig. 2 (a) shows a single line diagram where a SSSC is placed between buses  $i$  and  $j$ . The equivalent circuit of the system is shown in Fig. 2 (b), where the SSSC is represented by a synchronous voltage source  $\mathbf{V}_s$ . Reactance  $X_L$  represents the sum of  $X_{L1}$ ,  $X_{L2}$ , and transformer leakage reactance. The controllable parameter of the SSSC is  $V_s$ , which in fact represents the magnitude of the injected voltage  $\mathbf{V}_s$ , and may be positive or negative (oppose phase). In [9] the transmission characteristics for active and reactive powers were derived; summarizing them, the following mathematical formulations can be reproduced:

$$P_{ij} = -P_{ji} = P_o \times \left( 1 + \frac{V_s}{\sqrt{V_i^2 + V_j^2 - 2V_i V_j \cos \theta_{ij}}} \right) \quad (4)$$

$$Q_{ij} = Q_o^{ij} \times \left( 1 + \frac{V_s}{\sqrt{V_i^2 + V_j^2 - 2V_i V_j \cos \theta_{ij}}} \right) \quad (5)$$

$$Q_{ji} = Q_o^{ji} \times \left( 1 + \frac{V_s}{\sqrt{V_i^2 + V_j^2 - 2V_i V_j \cos \theta_{ij}}} \right) \quad (6)$$

where:

$$\theta_{ij} = \theta_i - \theta_j$$

$$P_o = \frac{V_i V_j}{X_L} \sin \theta_{ij}$$

$$Q_o^{ij} = \frac{V_i}{X_L} (V_i - V_j \cos \theta_{ij})$$

$$Q_o^{ji} = \frac{V_j}{X_L} (V_j - V_i \cos \theta_{ij})$$

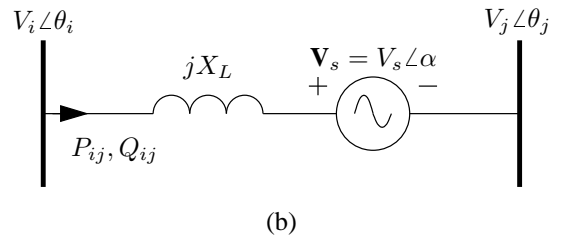
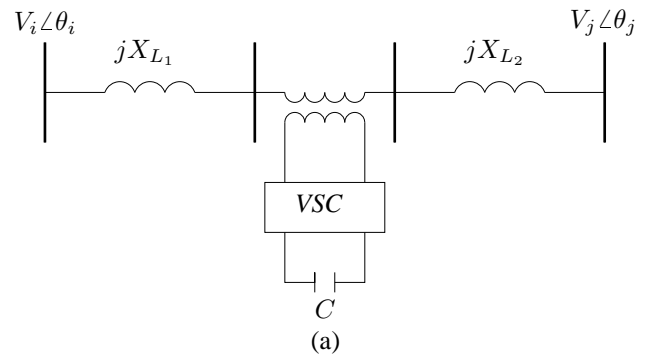


Fig. 2. (a) SSSC installed between buses  $i$  and  $j$ , (b) Equivalent circuit.

Equations (4)-(6) suggest that by proper control of  $V_s$ , steady-state active and/or reactive power flows in the line could be kept in specified values. Moreover, during transients, the SSSC can be used to damp electromechanical oscillations improving the overall dynamic performance of the system.

#### B. POD Controller

In order to damp oscillations and so enhance the small-signal angle stability of the system, a SSSC must be equipped with a stabilizer, similar to the PSS controllers, usually referred in the literature as power oscillation damping (POD) controller [2], [4], [10]. The selection of an appropriate input signal is a fundamental issue in the design of an effective and robust POD controller. Aiming to avoid additional costs associated with communication systems and to improve reliability of a POD controller, local signals are always preferred as input signal. Here, the active power flow through the SSSC ( $P_{Line}$ ) will be employed. Fig. 3 shows the SSSC control system diagram for damping electromechanical oscillations [9]. In the figure,  $V_o$  denotes the output of other SSSC control (e.g., power flow or line reactance controls) and determines the steady-state value of  $V_s$ .

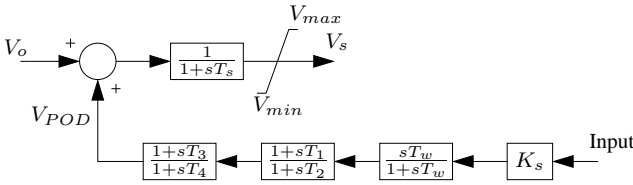


Fig. 3. Structure of SSSC controller for oscillation damping.

#### IV. SINGLE MACHINE INFINITE BUS SYSTEM

In order to verify the performance of PSS and SSSC controllers for damping local oscillations, two scenarios were considered for the single machine infinite bus (SMIB) system depicted in Fig. 4: system without SSSC (Scenario A); and system with SSSC compensating 30% of the line series reactance (Scenario B). The generator has a 3<sup>th</sup> model and the automatic voltage regulator is represented by a first-order transfer function.

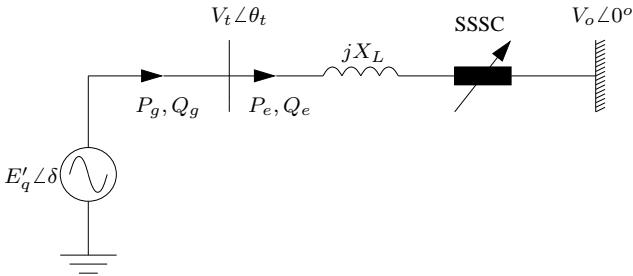


Fig. 4. SMIB with a SSSC.

The base operating point corresponds to a situation in which the generator delivers 0.6 p.u. of active power to the infinite bus. Table I provides the electromechanical mode characteristics for Scenarios A and B at  $\mu = 0.6$  p.u.. As can be seen, for Scenario A the system is unstable, whereas for Scenario B the system is stable but the electromechanical

mode is poorly damped. In view of that, two solutions, one in each scenario, were employed to provide adequate damping to the oscillations. For the Scenario A the addition of a PSS controller to the excitation system of the generator was adopted. For the Scenario B, a POD controller was applied to modulate  $V_s$  and so providing adequate damping torque at the generator shaft.

TABLE I  
Electromechanical mode characteristics at 0.6 p.u.

Scenario	Eigenvalue	Frequency [Hz]	Damping [%]
A	$+ 0,056 \pm j5,32$	0.84	- 1.0
B	$- 0,014 \pm j5,30$	0.84	+ 0.2

#### A. Design of PSS and POD Controllers

PSS and POD controllers' design is here based on Nyquist plots of a proper chosen Open Loop Transfer Function (OLTF). For the PSS design, the OLTF to be analyzed is  $\Delta\omega(s)/\Delta V_{ref}(s)$ . Closed loop stability for the open-loop unstable system is obtained by ensuring a counter-clockwise encirclement of the -1 point by the Nyquist plot of the OLTF after feedback compensation. The reader is referred to [10], [11], [12], for additional information regarding the frequency response design methods used in this paper. The Nyquist plot of Fig. 5 shows that the lead-lag blocks should provide about 34° of phase advance at the critical frequency of 5.32 rad/s. The PSS gain is adjusted to provide 10% of damping to the electromechanical mode. The Nyquist plot of the OLTF  $\Delta\omega(s)/\Delta V_{ref}(s)$  with the  $PSS_1(s)$ , given by (7), is shown in Fig. 6.

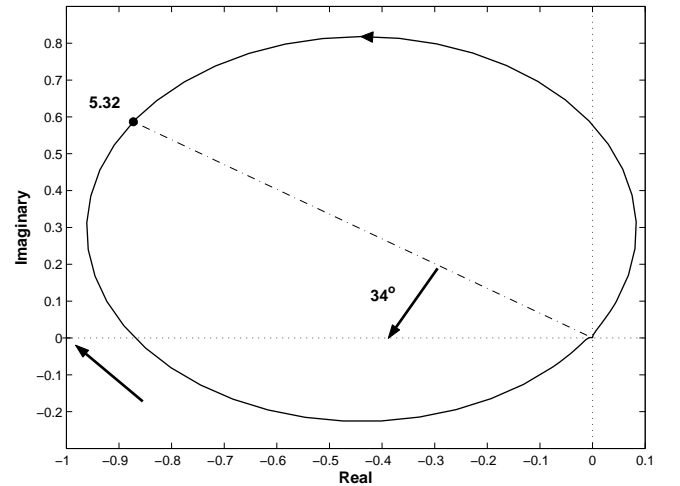


Fig. 5. Nyquist plot of  $\Delta\omega(s)/\Delta V_{ref}(s)$ .

For the POD design, the OLTF to be analyzed is  $\Delta P_{Line}(s)/\Delta V_{POD}(s)$ . Fig. 7 presents the Nyquist plot of the uncompensated OLTF. In this case (open loop stable system), the phase to be compensated is calculated to place the uncompensated loop of Fig. 7 as far as possible from the instability point -1. Hence, the critical frequency point is relocated to the real axis through a lag of 95°. Then, the POD gain is progressively increased to achieve the desired damping ration (10% in this case) obtaining the compensated

loop of Fig. 8. The transfer function of the POD designed is given by (8).

$$PSS_1(s) = 4.1 \frac{10s}{1+10s} \left( \frac{1+s0.254}{1+s0.139} \right)^2 \quad (7)$$

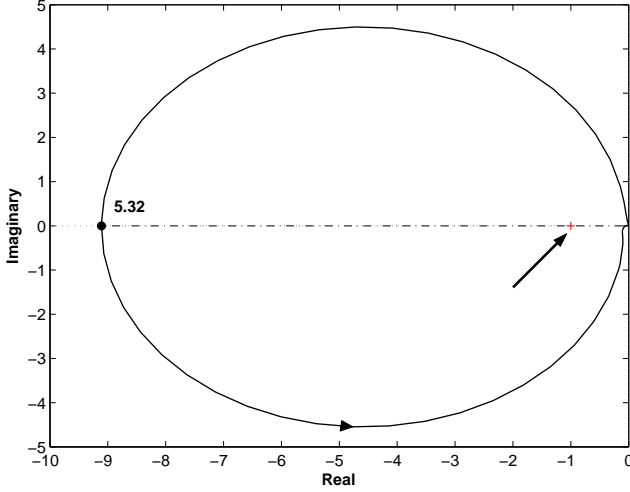


Fig. 6. Nyquist plot of  $\Delta\omega(s)/\Delta V_{ref}(s).PSS_1(s)$ .

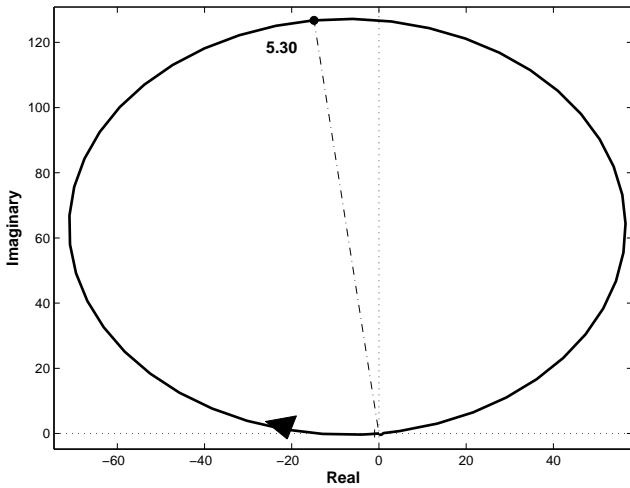


Fig. 7. Nyquist plot of  $\Delta P_{Line}(s)/\Delta V_{POD}(s)$ .

$$POD_1(s) = 2.0 \frac{10s}{1+10s} \left( \frac{1+s0.072}{1+s0.500} \right)^2 \quad (8)$$

#### B. Assessment of Stabilizers Effectiveness

The effectiveness of the stabilizer  $PSS_1(s)$  is verified from the step response plot of Fig. 9 and from the plot of Fig. 10 which shows the real part of critical eigenvalues (a direct measure of the electromechanical mode damping) as the loading factor varies from 0.1 to 0.9 p.u.. In Fig. 10 it is observed that the damping is higher at all operating points when the generator is equipped with the PSS than otherwise. Also is noted that the PSS extends the stability limit of the system, since the Hopf bifurcation occurs at 0.55 and 0.81 p.u. for the generator without and with PSS, respectively.

The effectiveness of the stabilizer  $POD_1$  is assessed from the step response plots of Figs. 11 (a) and (b), and from

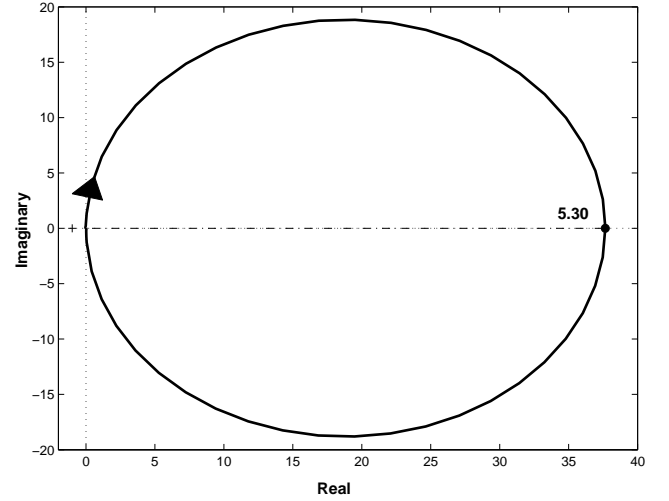


Fig. 8. Nyquist plot of  $\Delta P_{Line}(s)/\Delta V_{POD}(s).POD_1(s)$ .

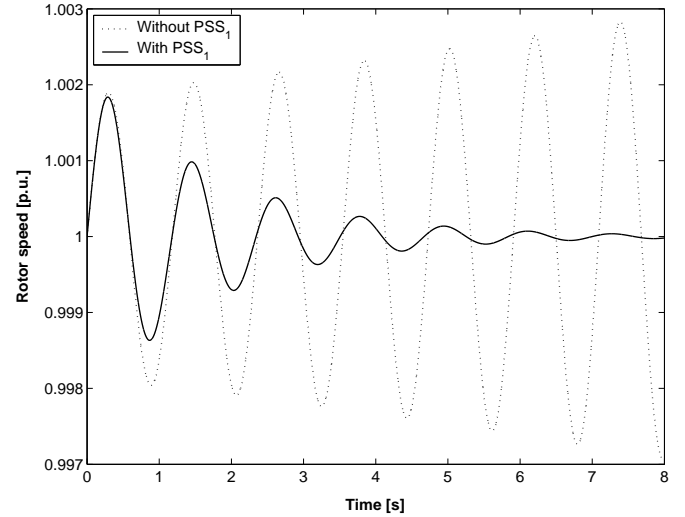


Fig. 9. Step response at 0.6 p.u..

the plot of Fig. 12 where is verified that the POD provides a superior damping to the electromechanical mode and extends the stability limit to 1.04 p.u., whereas without POD the system becomes unstable at 0.63 p.u.. The stability limits obtained in this section are summarized in Table II.

**TABLE II**  
Stability limits in p.u..

Scenario A	0.55
Scenario A - $PSS_1$	0.81
Scenario B	0.63
Scenario B - $POD_1$	1.04

#### V. MULTI-MACHINE SYSTEM

In order to investigate the effectiveness of PSS and SSSC controllers for damping inter-area oscillations, it was used the test system pictured in Fig. 13. This system, taken from [1] (and slightly modified), consists of two similar areas connected via a weak tie line. Here, the four generators has

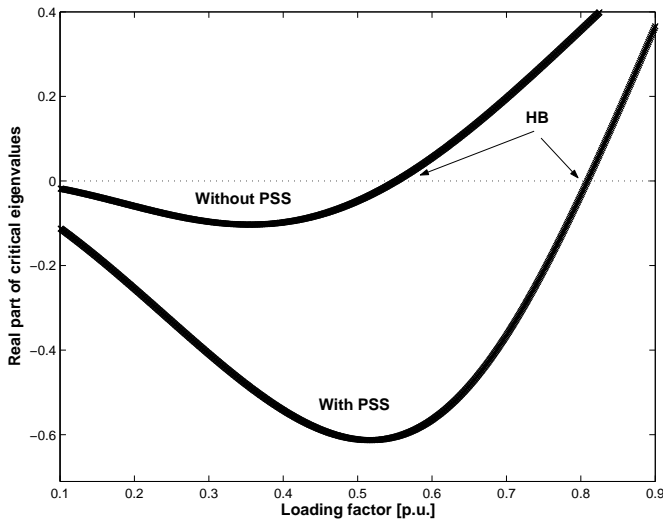


Fig. 10. Real part trajectory of critical eigenvalues.

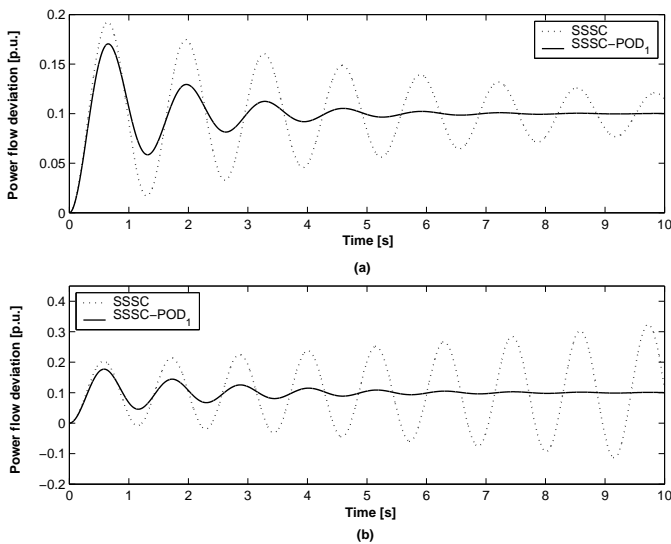
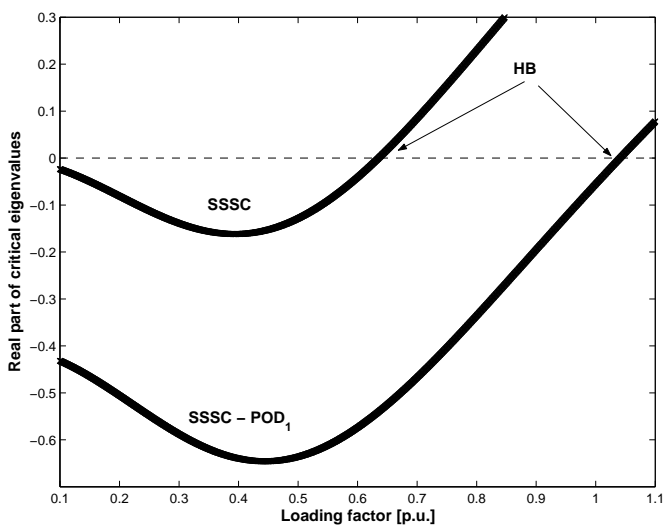
Fig. 11. Step response: (a)  $\mu = 0.4$  p.u., (b)  $\mu = 0.7$  p.u..

Fig. 12. Real part of critical eigenvalues.

a 4<sup>th</sup> model, all of them equipped with an automatic voltage regulator represented by a first-order transfer function. The

system exhibits three electromechanical oscillation modes; two local modes, one in each area, and one inter-area mode, in which the generating units in one area swing coherently and against the generating units located in the other area. Initially, two scenarios were analyzed: system without SSSC (Scenario C), and system with SSSC compensating 40% of the tie line series reactance (Scenario D). The base case considered here, where  $\mu = 1.0$  p.u., is the operating point considered in [1]. Tables III and IV show the electromechanical modes characteristics at 1.0 p.u. for Scenario C and D, respectively.

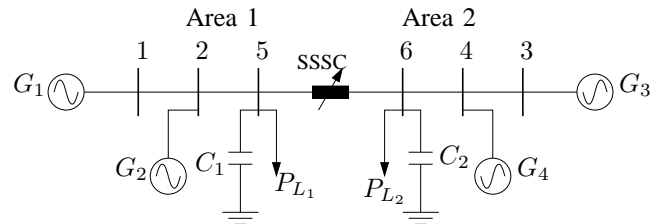


Fig. 13. Two-area test system with a SSSC.

TABLE III

Electromechanical modes characteristics for Scenario C.

Mode	Eigenvalue	Frequency [Hz]	Damping [%]
Local 1	$-0.892 \pm j7.63$	1.22	+11.61
Local 2	$-0.811 \pm j7.90$	1.26	+10.21
Inter-area	$+0.025 \pm j2.76$	0.44	-0.91

TABLE IV

Electromechanical modes characteristics for Scenario D.

Mode	Eigenvalue	Frequency [Hz]	Damping [%]
Local 1	$-0.883 \pm j7.65$	1.23	+11.46
Local 2	$-0.802 \pm j7.94$	1.27	+10.04
Inter-area	$+0.002 \pm j3.16$	0.50	-0.05

In both scenarios it is seen that the local modes (1 and 2) have acceptable damping (about 10%). It is important to note that the SSSC placed in the tie line has insignificant impact in the damping of such modes. Also note that, although be unstable in Scenario D, the inter-area mode has been almost stabilized by the series compensation done by SSSC. Two solutions, one in each scenario, were considered to provide appropriate damping for the inter-area mode. For the Scenario C, this is accomplished by PSSs added to the excitation system of the generators. For the Scenario D, a POD is employed to modulate the SSSC series voltage during transients in such a way that the oscillations be damped out.

Transfer function of PSSs used in the simulations is presented in (9). PSS gains were selected so as to provide 10% of damping for electromechanical mode at 1.0 p.u.. Step response results shown in Fig. 14 help evaluate the performance of the  $PSS_2$ . The applied disturbance is a 10% step in the mechanical power of the generator 1. Fig. 15 shows the eigenvalues loci as the loading factor is varied from 1.0 to 1.25 p.u.. It is noted that, beyond damping inter-area mode, the PSSs also contribute to a better damping of local modes. Observe that the occurrence of a Hopf bifurcation is associated to the inter-area mode. In Fig. 16 is possible to

realize that it occurs at 1.22 p.u..

$$PSS_2(s) = 33 \frac{10s}{1+10s} \left( \frac{1+s0.05}{1+s0.02} \right) \left( \frac{1+s3.0}{1+s5.4} \right) \quad (9)$$

Equation (10) gives the transfer function of the POD controller employed in the Scenario D, which was designed to provide 10% of damping to the electromechanical mode. Fig. 17 presents a step response results when is applied the same disturbance considered at Scenario C. In the figure is observed the good performance of the stabilizer  $POD_2$ . Note from Fig. 18 that, for this case (Scenario D), the occurrence of Hopf bifurcations is associated to the local mode 2. It is also possible to realize that the  $POD_2$  has no impact on local modes. Fig. 19 shows that Hopf bifurcation occurs at 1.72 p.u., that is, in a much higher loading factor than in the case when the damping of the inter-area mode was provided by the  $PSS_2$ , as summarized in Table V.

$$POD_2(s) = 3.15 \frac{10s}{1+10s} \left( \frac{1+s0.132}{1+s0.762} \right)^2 \quad (10)$$

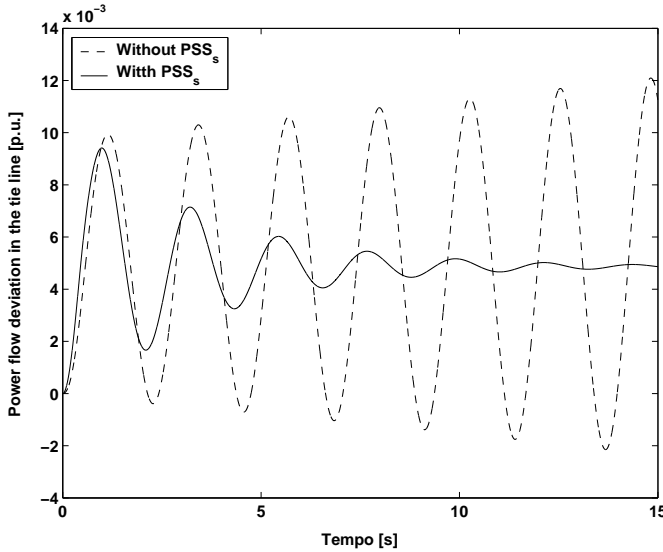


Fig. 14. Step response at 1.0 p.u..

Another possible scenario (Scenario E), in order to provide better damping and extend the small-signal rotor angle stability limit of the system, is to use the PSSs mainly to damp the local modes and the SSSC (equipped with POD) to damp the inter-area mode. Fig. 20 shows that for such scenario the occurrence of Hopf bifurcation is associated to the inter-area mode at 1.88 p.u. as can be seen in Fig. 21. An important remark is that has not been observed any adverse interaction among  $PSS_2$  and  $POD_2$  controllers.

TABLE V

Stability limits in p.u..

Scenario C - PSSs	Scenario D - POD
1.22	1.72

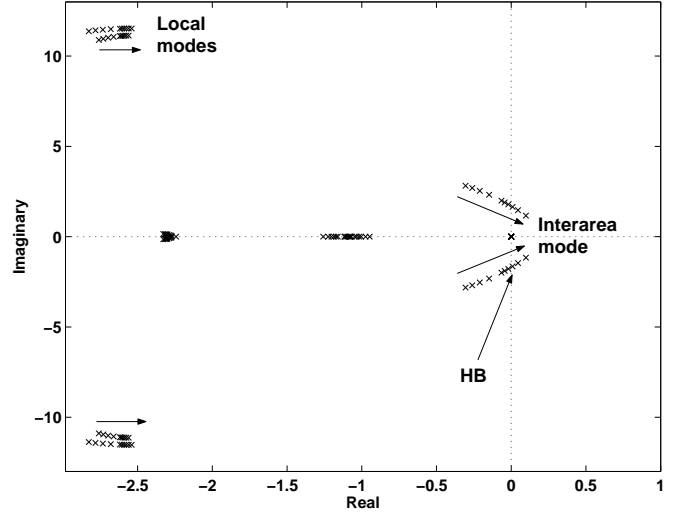


Fig. 15. Eigenvalues loci.

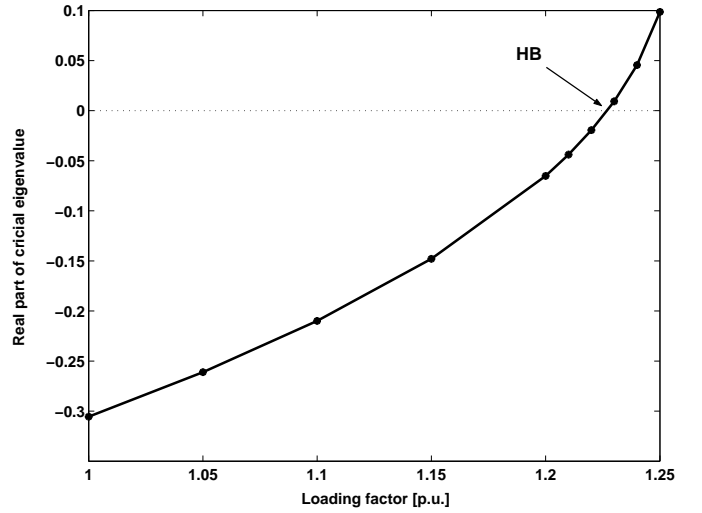


Fig. 16. Real part of critical eigenvalue.

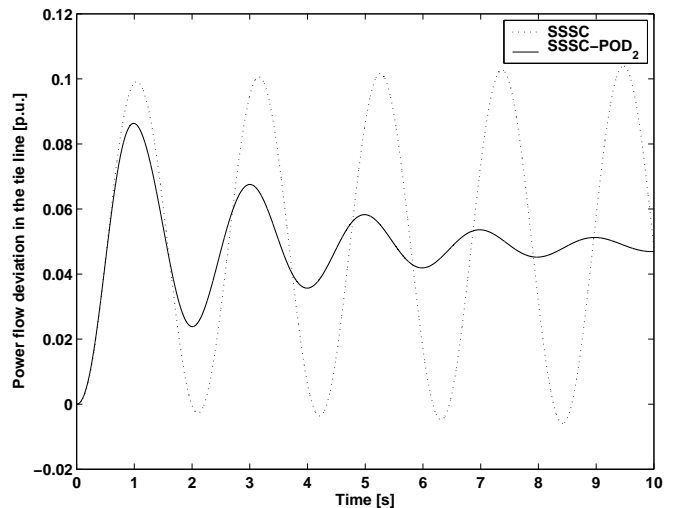


Fig. 17. Step response at 1.0 p.u..

## VI. CONCLUSION

This paper investigates the performance of PSSs and SSSC controllers for damping power system oscillations. The analy-

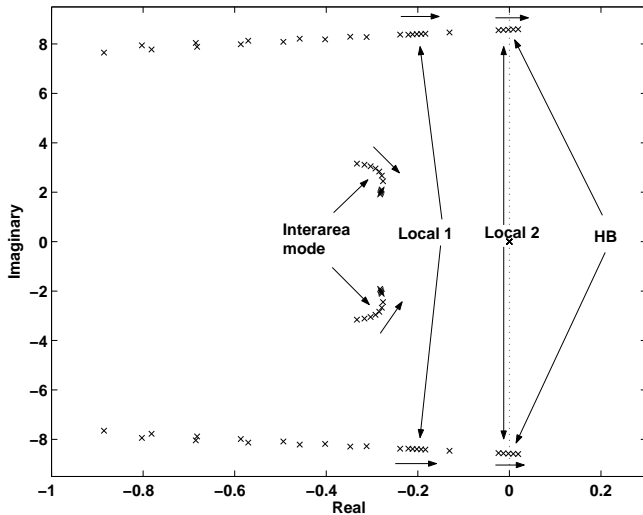


Fig. 18. Eigenvalues loci.

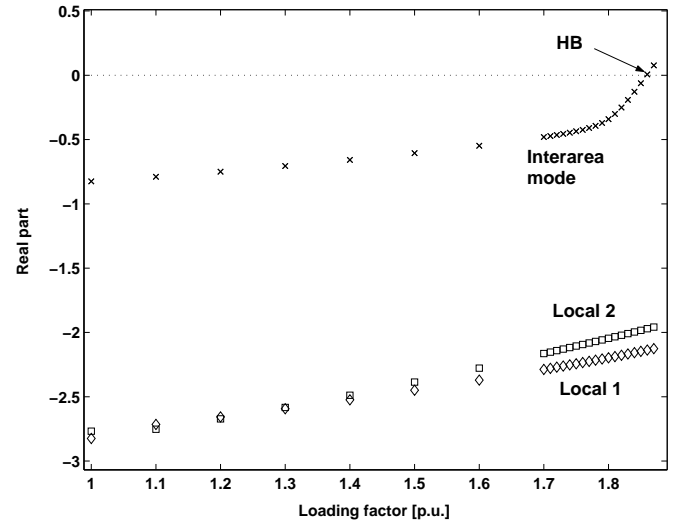


Fig. 21. Real part of critical eigenvalues.

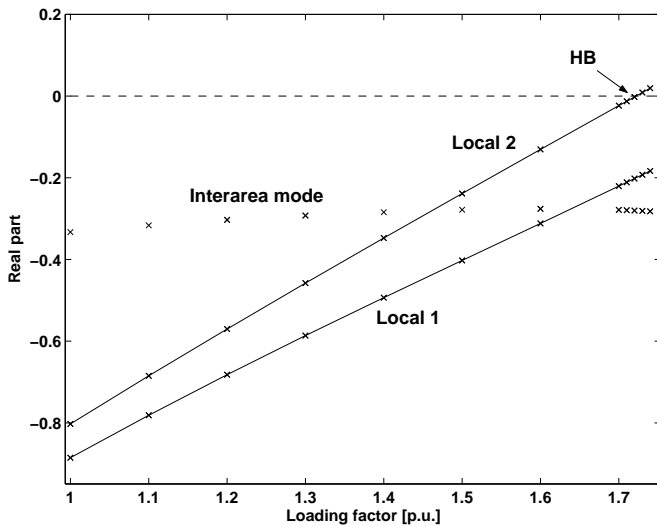


Fig. 19. Real part of critical eigenvalues.

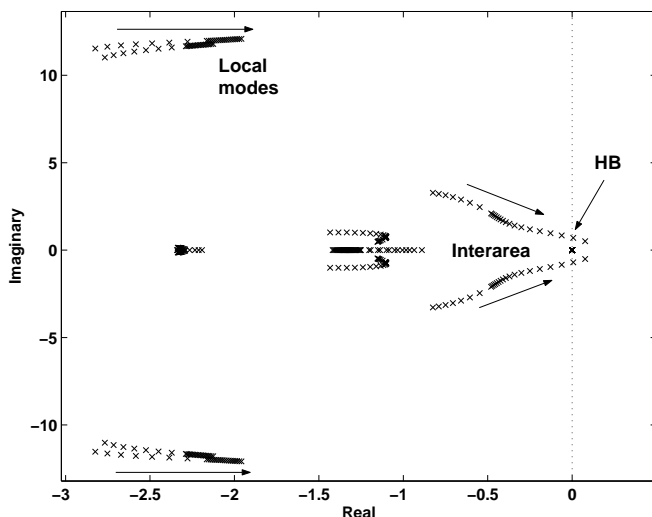


Fig. 20. Eigenvalues loci.

sis and design of controllers (PSSs and PODs) are based on modal analysis, Hopf bifurcations, and time and frequency response techniques. The results presented reveal that the

high electronic based controller, SSSC, provides better effectiveness on keeping small-signal rotor angle stability than the PSSs. Mainly, in the multi-machine system, the SSSC has presented a much better performance than the PSSs.

Although further investigations are required, the results presented in Section V have shown that PSSs and SSSC controllers could work together in an harmonious way to damp power system electromechanical oscillations.

Even though SSSC controller considerably increases the small-signal angle stability limits, a careful cost-benefit study must be taken into account when the use of this FACTS controller for damping power system oscillations is considered, because of its relatively high costs when compared to PSSs.

#### ACKNOWLEDGEMENT

The authors are grateful to CNPq for the financial support.

#### REFERENCES

- [1] P. Kundur, *Power System Control and Stability*. Editora Mc Graw-Hill, 1994.
- [2] L. J. Cai and I. Erlich, "Simultaneous coordinated tuning of PSS and FACTS controller for damping power system oscillations in multi-machine systems," *IEEE Power Tech Conference Proceedings*, vol. 2, pp. 136–141, 2003.
- [3] E. V. Larsen and D. A. Swann, "Applying power system stabilizers, part i: General concepts, part ii: Performance objectives and tuning concepts, part iii: Practical considerations," *IEEE Power Appar. Syst.*, vol. PAS-100, no. 12, pp. 3017–3046, 1981.
- [4] Y. H. Song and A. T. Johns, *Flexible AC Transmission System (FACTS)*. The Institute of Electrical Engineers, 1999.
- [5] N. G. Hingorani and L. Gyugyi, *Concepts and Technology of Flexible AC Transmission Systems*. IEEE Press - Jon Wiley & Sons, 2000.
- [6] R. Seydel, *Practical Bifurcation and Stability Analysis: From Equilibrium to Chaos*. Second edition. New York: Springer-Verlag, 1994.

- [7] L. Gyugyi, "Dynamic compensation of AC transmission line by solid state synchronous voltage sources," *IEEE Trans. Power Delivery*, vol. 9, pp. 904–911, 1994.
- [8] P. Kumkratug and M. H. Haque, "Improvement of stability region and damping of a power system by using SSSC," *IEEE PES*, 2003.
- [9] M. S. Castro, *A Influência de Controladores FACTS na Estabilidade de Ângulo a Pequenas Perturbações de Sistemas Elétricos de Potência*. Tese de Mestrado FEEC/UNICAMP, 2005.
- [10] N. Martins, H. J. C. P. Pinto, and J. J. Paserba, "Using a TCSC for line power scheduling and system oscillation damping - small-signal and transient stability studies," *IEEE PES Winter Meeting*, vol. 2, pp. 1455–1461, 2000.
- [11] N. Martins and L. Lima, "Eigenvalue and frequency domain fo small-signal electromechanical stability problems," *IEEE Symposium on Application of Eigenanalysis and Frequency Domain Methods for System Dynamic Performance*, vol. Special Publication 90TH0292-3 PWR, pp. 17–33, 1990.
- [12] A. Elices, L. Rouco, H. Bourles, and T. Margotin, "Physical interpretation of state feedback controllers to damp power system oscillations," *IEEE Transactions on Power Systems*, vol. 19, no. 1, pp. 436–443, 2004.